Available online at www.sciencedirect.com
ScienceDirect
Physica A 387 (2008) 4440–4452
PHYSICA A
www.elsevier.com/locate/physa

Flow dimension and capacity for structuring urban street networks

Bin Jiang*

Department of Land Surveying and Geo-informatics, The Hong Kong Polytechnic University, Hung Hom, Kowloon, Hong Kong

Received 31 May 2007; received in revised form 11 February 2008
Available online 26 February 2008

Abstract

This paper aims to measure the efficiency of urban street networks (a kind of complex networks) from the perspective of the multidimensional chain of connectivity (or flow). More specifically, we define two quantities: flow dimension and flow capacity, to characterize structures of urban street networks. To our surprise, for the topologies of urban street networks, previously confirmed as a form of small world and scale-free networks, we find that (1) the range of their flow dimensions is rather wider than their random and regular counterparts, (2) their flow dimension shows a power-law distribution, and (3) they have a higher flow capacity than their random and regular counterparts. The findings confirm that (1) both the wider range of flow dimensions and the higher flow capacity can be a signature of small world networks, and (2) the flow capacity can be an alternative quantity for measuring the efficiency of networks or that of the individual nodes. The findings are illustrated using three urban street networks (two in Europe and one in the USA).

Keywords: Flow capacity; Flow dimension; Efficiency; Small worlds; Urban street networks

1. Introduction

Urban street networks can be seen as a connectivity graph from two different and contrasting perspectives. On the one hand, an urban street network is regarded as a graph with nodes and edges representing respectively the junctions and street segments (between two adjacent junctions). This can be called a geometric approach. On the other hand, a topological approach, in contrast to the geometric approach, regards an urban street network as a connectivity graph consisting of nodes representing individual named streets [16], and edges linking the nodes if the corresponding streets are intersected. The difference between the two approaches is subject to whether or not geometric distance plays an important role in the graph theoretical representations. For the geometric approach, the graph edges (street segments) are weighted by the distance between the two corresponding junctions. With the topological approach, an entire street is collapsed as a node, and all the edges have a unit weight [25]. In other words, there is no weighting difference among the edges. The geometric approach is an advantageous representation in conventional network analysis [12] and transportation modelling [20] with geographic information systems (GIS), but it is not suitable for illustrating the structure of urban street networks, since the structure captured by the geometric approach is pretty simple, i.e., 3 or 4 links for most road junctions.

* Tel.: +852 2766 4335; fax: +852 2330 2994.
E-mail address: bin.jiang@polyu.edu.hk.

0378-4371/$ - see front matter
doi:10.1016/j.physa.2008.02.047

The topological approach is a holistic approach that considers the interrelationship of individual streets for better understanding the underlying structure of urban street networks. This is consistent with human cognition of large-scale environments. For example, in conveying a direction from location A to B, we often refer to a number of named streets that constitute the path. Using MSN Maps & Directions (mappoint.msn.com), we can easily make a query from where you live to where you work. The returned direction or path would consist of a number of named streets attached with mileages. This appears to suggest that topology is primary (at a structural level), and geometry is secondary (at a detailed level). In fact, a city is indeed an interconnected whole consisting of paths, edges, districts, nodes and landmarks at a cognitive level [18]. In a similar fashion, a city can be perceived as an interconnected whole that links individual units [2]. These individual units or constituents have different geometric sizes and shapes, but they are all perceived individually as a perceivable unit at a structural level. Alexander's [2] "a city is not a tree" suggests that a city is neither a tree nor a regular lattice, but a semilattice with some shortcuts among some far-distant units. Interestingly enough, this semilattice structure resembles well the structure that we found in the topologies of urban street networks in terms of street–street intersection.

The topologies of urban street networks have an efficient structure, which is demonstrated by a variety of other biological, technological, and social networks. The structure is called a small world network that is an intermediate status between an order and disorder. It has a higher efficiency in the sense of transporting information, goods or viruses at both local and global levels, when compared to their regular and random counterparts. This view of high efficiency can be seen from two prominent properties of small world networks, i.e. a small separation and a high degree of clustering. In a social setting, a small separation implies that any two arbitrarily chosen persons A and B are linked by a short chain of intermediate persons. The person A knows someone, who knows someone, . . . who knows the person B, and the number of the someone is no more than 6. This is the so-called "six degrees of separation", which has been empirically verified by the well-known experiment conducted by Milgram [19]. It should be noted that the two persons A and B are randomly chosen from a large population, say, the entire population of the planet. On the other hand, small world networks tend to be highly clustered. It implies that friends of a friend are likely to be friends. From a point of view of information flow, information can be diffused very quickly from one to another globally, and it also spreads efficiently among the circle of the friends locally. Although we use social networks as an example, the efficient structure explained holds true for a wide variety of real world networks (for comprehensive surveys, refer to Refs. [1,21], or more recently, Refs. [7,23]). Small world networks help in explaining why computers can be infected overnight, and why the SARS virus can diffuse so quickly among the large population of human beings. The beauty of the small world networks lies on the fact that it retains an efficient structure inherited from their parents: regular and random networks (*cf.* Section 2 for more explanations).

This paper aims to measure network's efficiency or to characterize structural properties of urban street networks from the point of view of multidimensional chain of connectivity (or flow). This work is mainly inspired by the efficiency view of small world networks, in terms of how information flows among the nodes of a complex network. In this connection, Latora and Marchiori [17] suggested a new formulation of the small world theory. However, the formulation, actually current literature in small world networks, does not fully capture the structural complexity of real world networks. What has not drawn enough attention is the multidimensional chain of connectivity [10] for characterizing the structure of real world networks. The notion of multidimensional chain of connectivity, which is referred to as flow in the context of this paper, is a fundamental concept of Q-analysis [4] — a computational language for structural description. To illustrate the concept of flow, let us see how an innovation, which involves multiple expertise, diffuses among an organization or from one person to another. Clearly the innovation would diffuse among the individuals who have the multiple expertise. Different innovations involve different multiple expertise. Thus the social network of the organization forms a multidimensional chain of connectivity (or flow for simplicity) for different innovations to flow from one to another (*c.f.* Section 3 for more details).

With the concept of flow, we define two relevant quantities: flow dimension and flow capacity, to measure the efficiency of individual nodes or that of an entire network. The concept and quantities are applied to three urban street networks to illustrate some nice structural properties. To our surprise, for the topologies of urban street networks, previously confirmed as a form of small world and scale-free networks, we find that (1) the range of their flow dimensions is rather wider than their random and regular counterparts, (2) their flow dimension shows a power-law distribution, and (3) they have a higher flow capacity than their random and regular counterparts. The findings have far reaching implications for understanding the structure of urban street networks, whose topologies can be regarded a network infrastructure to service the flows of various kinds including vehicle, people, and goods.

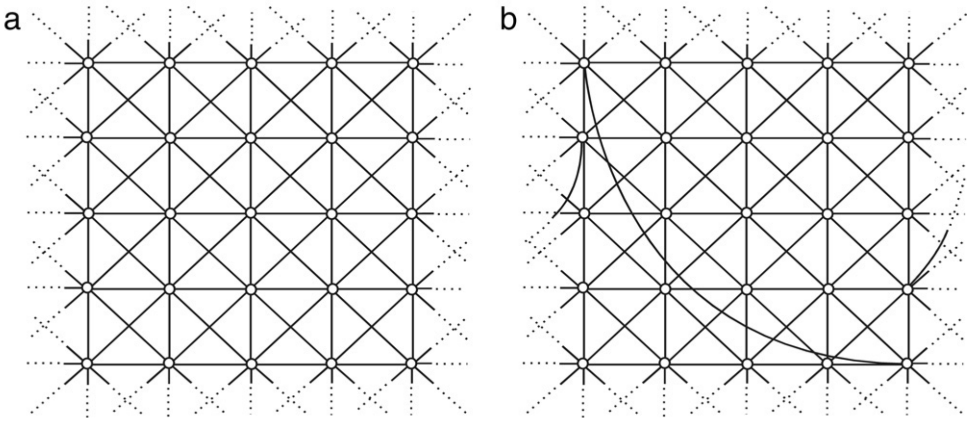

Fig. 1. Lattice (a) — a big world and semilattice (b) — a small world (Note: different from the initial Watts' model [27] and similar to Ref. [22], we randomly add a few new edges, but the new edges do not significantly change the average degree of the lattice).

The remainder of this paper is organized as follows. Section 2 introduces some basic mathematics of the small world and scale-free networks from a point of view of efficiency. Section 3 presents the concept and computation of flow using a simple notational street network. In Section 4, we report our major findings based on the computation of flow dimension and capacity for three urban street networks. Finally Section 5 concludes the paper and points to our future work.

2. Mathematics of small world and scale-free networks

To introduce small world networks, let us start with the big world of a lattice illustrated in Fig. 1(a). Imagine that this regular lattice is expanded to include up to hundreds of millions of nodes, so that it becomes obviously a very big world. Generally speaking, the (topological) distance from any node to any other node tends to be very large, as in general one has to travel node by node to reach one's destination. However the situation can be significantly tipped, if we add some new edges that bring some far-distant nodes together (a sort of shortcuts) as illustrated in Fig. 1(b). The shortcuts significantly shorten the distance from any node to any other node in general, so the lattice is transferred to a semilattice — a small world. To understand why the semilattice is a small world, we must introduce some basic mathematics of graphs and networks.

A graph $G(V, E)$ consists of a finite set of vertices (or nodes) $V = \{v_1, v_2, \ldots v_n\}$(where the number of nodes is n) and a finite set of edges (or links) E, which is a subset of the Cartesian product $V \times V$. The initial small world and scale-free networks are based on the connectivity graphs whose edges have neither directions nor weights. This kind of graph can be simply represented by an incidence matrix $\mathbf{R}(G)$, whose individual elements are defined by:

$$r_{ij} = \begin{cases} 1, & \text{if } v_i v_j \in E, \\ 0, & \text{otherwise.} \end{cases} \tag{1}$$

It is not difficult to note that the above incidence matrix $\mathbf{R}(G)$ is symmetric, i.e., $\forall r_{ij} \Rightarrow r_{ij} = r_{ji}$, and that all diagonal elements are equal to zero, i.e., $\forall r_{ij}|_{i=j} \Rightarrow r_{ij} = 0$. Thus the lower or upper triangular matrix of $\mathbf{R}(G)$ is sufficient for the description of the graph G. For a complete graph, in which every node links to every other, there are $n(n-1)/2$ edges. However, most real world networks are far sparser than a complete graph. If on average every node has m edges (average degree), then a sparse graph implies $m << n(n-1)/2$. The following two measures (or equivalently the initial small world and scale-free network models) are based on the undirected, unweighted, and connected graphs. However, this paper, or definition of flow dimension and capacity, has released the constraints. It implies that the concept of flow to be defined in what follows is applicable for directed, weighted and unconnected graphs as well.

Topological distance (or distance) is a basic concept of graph theory [9], and fundamental for small world networks as well. The distance $d(i, j)$ between two vertices i and j of a graph is the minimum length of the paths that connect the two vertices, i.e., the length of a *graph geodesic*. For a given graph, the length of the maximum graph geodesic is called *graph diameter*. The distance of a given vertex v_i far from all other vertices is called average path length. It is defined by

$$L(v_i) = \frac{1}{n-1} \sum_{j=1}^{n} d(i, j). \tag{2a}$$

The average ($\frac{1}{n} \sum_{i=1}^{n} L(v_i)$) of the average path length of the individual vertices is the average path length of the graph G,

$$L(G) = \frac{1}{n(n-1)} \sum_{i=1}^{n} \sum_{j=1}^{n} d(i, j). \tag{2b}$$

From the equations, we might have a better sense of understanding of why the above lattice tends to be a big world. It is because that the average path length of a graph is increased with the square of the number of nodes ($\sqrt{n}$), i.e., the more the nodes, and the longer the average path length. This is unlike the one-dimensional lattice whose path length is linearly increased. For a lattice that contains hundreds of millions of nodes, the average path length tends to be a large value. However, the introduction of some shortcuts into a large lattice can significantly reduce the average path length, and thus shrink the big world into a small one. Actually a random graph whose edges are randomly determined in terms of which node links to which node also has a short average path length according to random graph theory [8], first studied by Erdös and Rényi [11]. For a random graph, the average path length is increased very slowly (logarithmically) with the number of nodes, i.e., $L_{\text{random}} = \ln(n)/\ln(m)$, where m is the average degree of the graph. So in terms of average path length, a small world network is very similar to a random network, i.e., a small separation between two arbitrarily chosen nodes of the network. This implies that a small world network has a very efficient structure for information flow at a global level.

Information flows efficiently not only at the global level, but also at a local level, i.e., in the circle of immediately neighbouring nodes. Again with the lattice in Fig. 1a, every node has eight neighbouring nodes. If the eight nodes all have an edge with each other (being a complete graph), then there would be in total $A_8^2 = 28$ possible edges. But actually there are only 12 edges as we can see. The ratio $12/28 = 0.43$ indicates the degree of clustering for the eight neighbouring nodes, i.e., the higher the ratio, the more efficient the information that flows among the neighbours. Obviously the highest value of the ratio is 1, when the neighbours are highly connected as a complete graph, i.e. every node links to every other node. From the information flow point of view, the highly connected complete graph has a maximum efficiency. This can be seen from our daily lives. If all of my friends are friends with one another, then information about me can be spread maximally among the circle of my friends. In reality, friends of a person are hardly fully connected as a complete graph, BUT any two of the friends are *likely* to be friends in general. This implies a high clustering degree for a person or a social network in general. The clustering degree is measured by the clustering coefficient [27] that can be formally defined by,

$$C(v_i) = \frac{\text{\# of actual edges}}{\text{\# of possible edges}}. \tag{3a}$$

The average ($\frac{1}{n} \sum_{i=1}^{n} C(v_i)$) of the clustering coefficient of the individual vertices is the clustering coefficient of the graph G,

$$C(G) = \frac{1}{n} \sum_{i=1}^{n} \frac{\text{\# of actual edges}}{\text{\# of possible edges}}. \tag{3b}$$

For an equivalent random graph (which means a graph having the same size and the same average degree as a random graph), its clustering coefficient is equal to the probability that two randomly selected nodes get connected, i.e., m/n. The ratio of m to n tends to a very small value (as a reminder, we are dealing with large sparse graphs). However, for an equivalent regular graph, its clustering coefficient tends to be a big value, given by $C_{\text{lattice}} = 0.43$. In summary, both the average path length and clustering coefficient can be good indicators for the efficiency of a real network respectively at the global and local levels, i.e. $E_{\text{glob}}(G) = 1/L(G)$, $E_{\text{loc}}(G) = C(G)$ [17].

The high efficiency of small world networks comes from an important fact that for most real networks like the Internet, the connectivity is unevenly distributed among the nodes. In other words, connectivity is not randomly

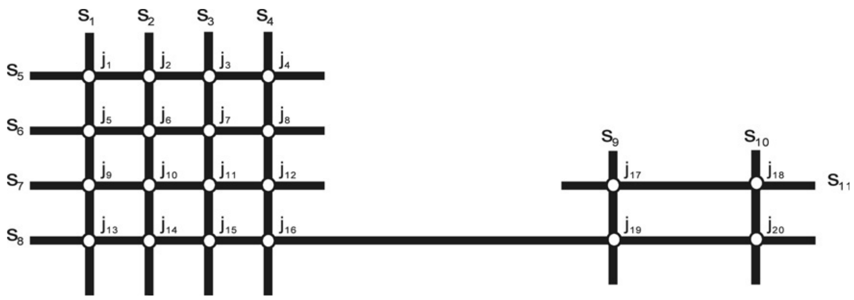

Fig. 2. A notional street network.

decided. A very few nodes are far more connected than the rest of others, i.e. vital few versus trivial majority. The highly connected nodes are called hubs. This special category of small world networks is called scale-free networks [5], which can explain why a small world is a small world. This is because of the existence of hubs. It also helps to understand the nature of dynamics and evolution of many real world networks. It is important to note the relationship between the small world networks and scale-free networks. In general, a scale-free network is certainly a small world, but not vice verse. Small world networks can be put into different categories in terms of the nature of connectivity distribution [3], and they all appear to have an efficient structure. In the next section, we will introduce the concept of flow for better characterizing the efficiency of networks or of individual nodes.

3. Defining the concept of flow: Dimension and capacity

Having introduced small world networks from the point of view of information flow, in this section we attempt to define the concept of flow. Flow is often referred to as movement of energy, material or information from one place to another through complex networks. In reality, there are different kinds of flows, such as vehicle flows, information flows, and flows of innovations, rumours and viruses. However, flow in the context of this paper is defined as the multidimensional chain of connectivity, referring to alternative channels, i.e., the number of liaison actors between a pair of actors. It aims to characterize structural efficiency of individual nodes in a network or that of the network as a whole. How efficient a street network, or a street within the network, is in its capacity to accommodate/convey people or vehicle movement is subject to the underlying structure. The structure can be characterized by two flow related quantities: flow dimension and flow capacity.

For the sake of convenience and simplicity, but without loss of generality, we adopt a notional street network for illustration of the concept and computation of flow. The notional street network consists of 11 streets (s_1–s_{11}) and 20 junctions (j_1–j_{20}) (Fig. 2). If we concentrate on the two pairs of streets $\langle s_1, s_4\rangle$ (in fact any pair from the set $\langle s_1, s_2, s_3, s_4\rangle$, or equivalently any pair from the set $\langle s_5, s_6, s_7, s_8\rangle$) and $\langle s_9, s_{10}\rangle$, clearly the former pair has four other streets cutting across, while the latter has only two streets cutting across. It appears that the left lattice is more efficient than the right one in transporting people or vehicles. This observation provides a basic inspiration to develop the quantities for characterizing the structural property of a network, or that of individual nodes with the network.

To further illustrate the concept of flow, we represent the notional street network topologically by taking individual streets (s_1–s_{11}) as nodes and street intersections as links of a connectivity graph (Fig. 3a). This connectivity graph is actually derived from a street–street incidence matrix S(*cf.* matrix (A.1) in the Appendix) (Note: the matrix S is still symmetric, but in more general, it can be asymmetric, representing a bigraph). To see how much flow there is between each pair of streets, we compute the flow matrix using the operation $FS = S * S'$ (*cf.* matrix (A.2) in the Appendix). The flow matrix can be represented as a flow graph in Fig. 3b, where edge thickness represents flow dimensions. As a reminder, what FS represents is the number of liaison nodes (acting as a liaison role) between every pair of nodes. It should not be confused with the number of walks of length 2, which is obtained by $S * S$, connecting nodes i and j, although they are same due to the symmetric nature of matrix S in this simple example. Up to this point, the reader may have found that the concept of flow is a bit "counter-intuitive", because the links in Fig. 3a are not retained in Fig. 3b. Our goal is to develop new metrics that can be used to measure structural efficiency of a network or its individual nodes from the perspective of multidimensional chain of connectivity (or the flow we refer to). More specifically, we want to characterize the structural efficiency based on Fig. 3b (alternative novel representation) rather than Fig. 3a (conventional representation). This is a unique feature of our model.

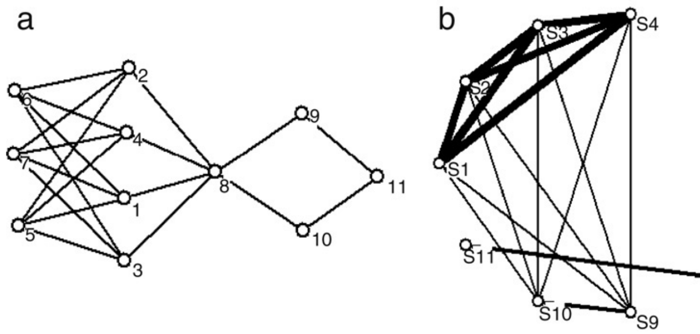

Fig. 3. The topology of the notional street network (a), and its flow graph (b) (Note: flow dimension is indicated by edge thickness with respect to 1, 2, and 4 with the figure b).

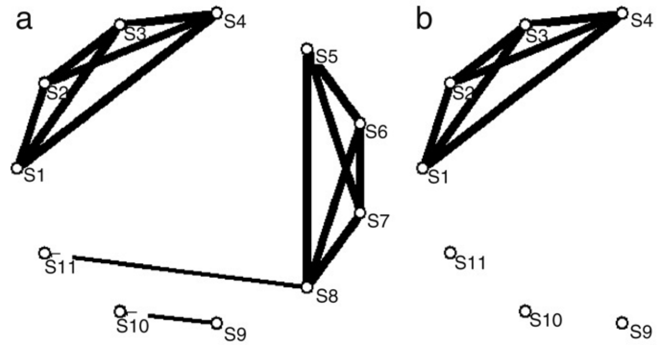

Fig. 4. Slicing the flow graph at the dimensions of two (a) and four (b).

The flow dimension refers to the number of liaison streets shared by a pair of streets, i.e., a sort of intersection strength between the pair. For instance, the pair $\langle s_1, s_4 \rangle$ has four common streets (i.e., s_5, s_6, s_7 and s_8), while the pair $\langle s_9, s_{10} \rangle$ has just two liaison streets. The magnitude of flow dimension reflects the degree of flow between a pair of streets. Taking a path s_2–s_3–s_9 for example, the first half path (s_2–s_3) is very wide, while the second half path (s_3–s_9) very narrow. This flow graph is the starting point to define flow capacity. For the purpose of defining and computing the flow capacity, we slice the flow graph at different dimensional levels. First the flow graph itself represents the situation at dimension one, i.e, all edges above the dimension one are retained. We can filter out those edges whose flow dimension is less than one, and less than two, respectively. In the end, flow graphs at dimension two (Fig. 4a) and four (Fig. 4b) are formed. This slicing technique is taken from Q-analysis, and it is also given other names such as *m*-cores [26], or *m*-slices [24] in social network analysis.

Before formally defining the concept of flow capacity, we assume the sliced flow graphs serve as a network infrastructure for information flows. The flow graphs at lower dimensions can only transport low-dimensional information, while the higher-dimensional information needs higher flow graphs. This has an analogy to the different lanes of a street. For instance, bicycles can ride in a car lane, but cars cannot drive in a bicycle lane. The bicycles and cars are in analogy with lower-dimensional and higher-dimensional information in this case. Therefore the flow graph in Fig. 3(b) can only diffuse one-dimensional information flows, and the flow graph in Fig. 4(b) can diffuse four-dimensional information flows. Flow capacity is defined as a ratio of flow width to flow length. Taking the node s_1 for example, its flow capacity at dimension one with respect to Fig. 3b can be expressed by $\sum_{j=2}^{11} \frac{1}{d_1(1,j)} = 5$. With the expression, the numerator indicates dimension one and denominator represents the flow length (which is the shortest distance) from the particular node to all others. Clearly, the subscript of d indicates dimension one. At dimensions two and four (with respect to Fig. 4a and b), flow capacities are computed by $\sum_{j=2}^{11} \frac{2}{d_2(1,j)} = 6$ and $\sum_{j=2}^{11} \frac{4}{d_4(1,j)} = 12$. It should be noted that the flow graphs at dimensions three and four are identical. So the flow capacity at dimension three is computed by $\sum_{j=2}^{11} \frac{3}{d_3(1,j)} = 9$. The sum of the four flow capacities is the flow capacity of the node s_1, i.e.,

$(5 + 6 + 9 + 12)$. To get rid of the size effect, the sum is divided by $11 * (11 - 1)$, so in the end the flow capacity of the node is $(5 + 6 + 9 + 12)/(11 * (11 - 1)) = 0.29$.

Having illustrated the computation of flow capacity with the example, we can remark that there are two factors that decide the flow capacity. One is called flow dimension and the other is called flow length (actually distance of geodesic at different dimensional levels). Intuitively, a higher flow dimension and a shorter flow length lead to a higher flow capacity. In general, for a vertex v_i, its flow capacity is defined by

$$FC(v_i) = \frac{1}{(n-1)} \sum_{k=1}^{\ell} \sum_{j=1}^{n} \frac{k}{d_k(i, j)} \tag{4a}$$

where ℓ is the highest-dimensional level.

The average of the flow capacity of the individual vertices is the flow capacity of the graph G,

$$FC(G) = \frac{1}{n(n-1)} \sum_{i=1}^{n} \sum_{k=1}^{\ell} \sum_{j=1}^{n} \frac{k}{d_k(i, j)}. \tag{4b}$$

It is important to note that the above definition is illustrated with an undirected, unweighted and connected graph, but it holds true for a directed, weighted, and unconnected graph as well. Obviously a complete graph has the biggest flow capacity, since every node has the biggest flow dimension on the one hand, and the smallest flow length from every node to every other on the other hand. It should be noted that so far the flow capacity is defined as a measure for individual streets and the network of the streets. For the topological approach, both primal and dual approaches are transferable [6,13]. The above definition and computation can also be applied to the individual junctions of a street network. To achieve this, we must derive a street–junction incidence matrix first. Taking the notional street network for example, the street–junction matrix is represented as an incidence matrix of the size 11×20, namely SJ (see matrix (A.3) in the Appendix). Actually the previous street–street incidence matrix S can be derived using operation $S = SJ * SJ'$ (Note: the diagonal elements are set as zero, the same for the following matrix J). In the same fashion, we can derive the junction–junction incidence matrix J, i.e., $J = SJ * SJ'$ (see matrix (A.4) in the Appendix). Furthermore, using the junction–junction incidence matrix, the junction–junction flow matrix FJ can be derived (see matrix (A.5) in the Appendix). Based on the flow graph and using the above formulas, the flow capacity for the individual junctions and for the entire topology can be computed.

4. Computing the flow dimension and capacity for structuring urban street networks

We applied the concept and computation of flow to three urban street networks: Gävle (Sweden), Munich (Germany) and San Francisco (USA), including respectively 565, 785 and 637 streets – the same datasets used in our previous work [16]. The reader may notice from Fig. 5 that Munich is a natural (self-organized or self-evolved) city, and San Francisco an artificial (or planned) city, whereas Gävle is somewhere between the natural and artificial cities, in particular with reference to the fact that two neighbours of Gävle are surrounded by the ring roads. With the networks, we intend to illustrate some hidden structure or patterns, in comparison with their regular and random counterparts. The first step is to complete the transformation from a network to topology using the topological approach introduced at the beginning of the paper. Fig. 5(d) illustrates the topology transformed from the San Francisco street network. The second step is to derive the flow graphs based on the topologies, and further compute the flow capacity for the individual nodes and for the entire topology. Three major findings are derived from the experiments.

The first finding is that the range of flow dimensions of the topologies is extremely wider than that of their regular and random counterparts (Table 1). For instance, the Gävle topology involves 14 flow dimensions, while the number for its random and regular counterparts is only 2 and 3 (Table 2). This fact can be further illustrated through a special visualization of the topologies. Again, taking the Gävle case for example, we arrange the topology layer by layer in terms of flow dimensions, i.e., from the bottom of a lowest dimension to the top of a highest dimension. Fig. 6 demonstrates the fact of fourteen layers with the Gävle topology, and three layers with the random counterpart.

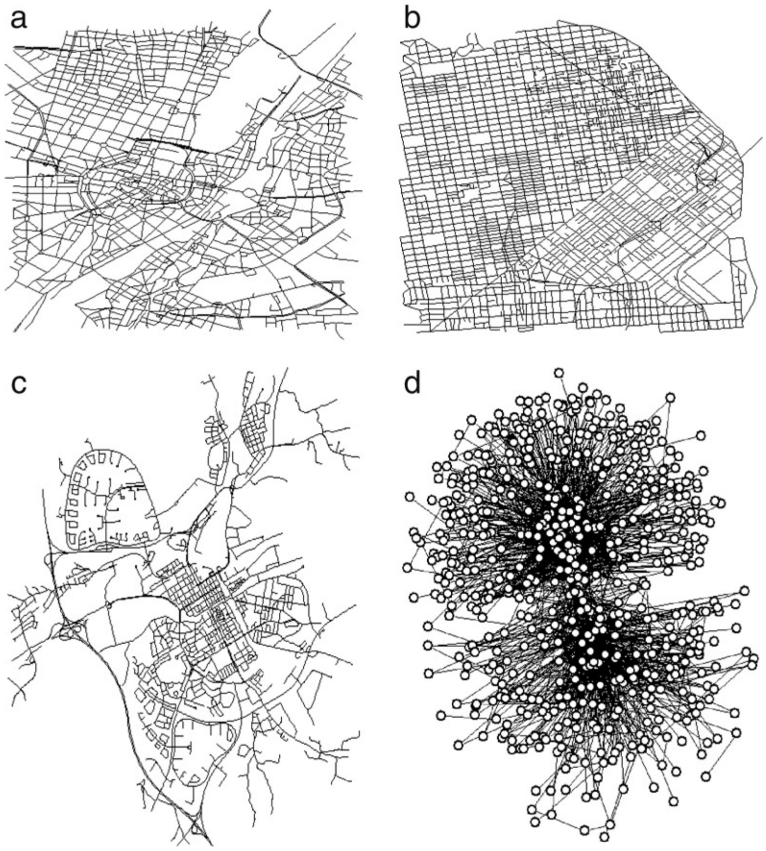

Fig. 5. Street networks of Munich (a), San Francisco (b), Gävle (c) and the San Francisco topology (d).

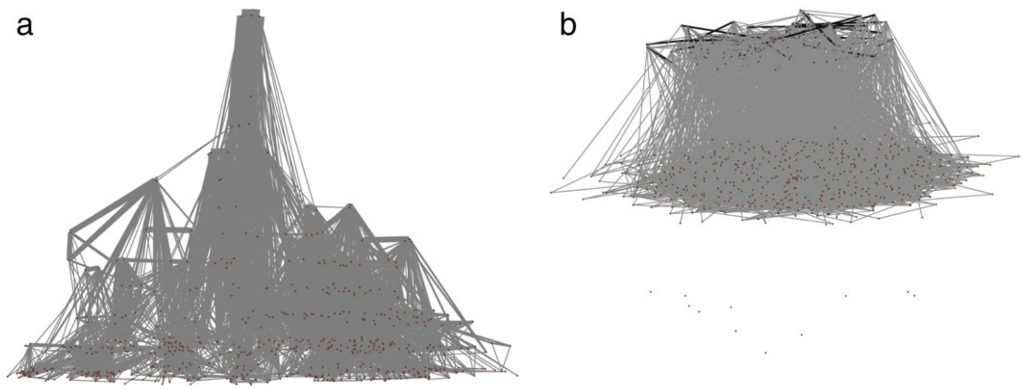

Fig. 6. Flow graphs of the Gävle topology (a) and its random equivalent (b).

Table 1
The range of flow dimensions for the three topologies and their counterparts (RF = the range of flow dimensions)

	Gävle	Munich	San Francisco
RF	14	11	46
RF-rand	2	2	3
RF-reg	3	4	7

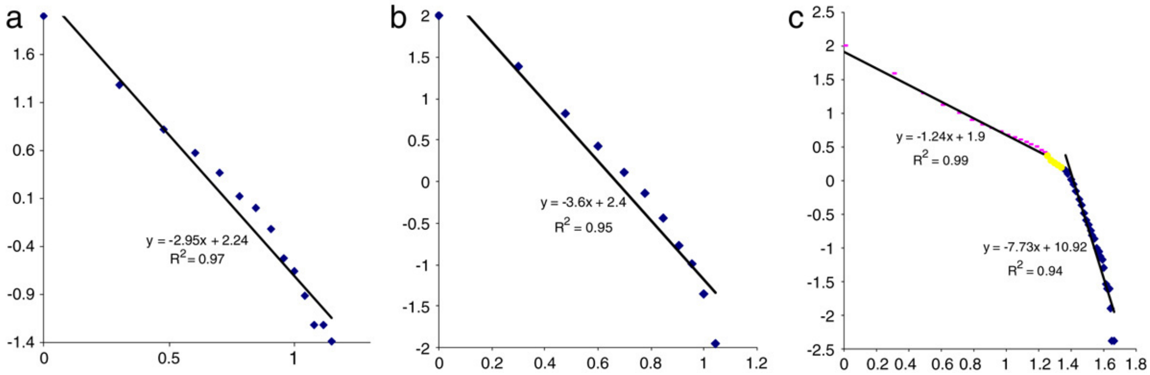

Fig. 7. Cumulative distributions of flow dimension of Gävle (a), Munch (b) and San Francisco (c) (The x-axes = flow dimension, and y-axes = cumulative probability).

Table 2
Flow capacity (FC) of the three networks in comparison to their counterparts (Note: n= size of networks, m= average degree)

	Gävle	Munich	San Francisco
FC	0.53	0.69	3.51
FC-rand	0.37	0.41	0.73
FC-reg	0.12	0.29	1.34
m	3.76	4.76	7.38
n	565	785	637

The second finding is that the flow dimension demonstrates a power-law distribution with different connectivity exponents: 2.9 for Gävle, 3.6 for Munich, 1.2 for one part of San Francisco and 7.7 for another part (see Fig. 7 for the log–log plots). This implies that most streets have a quite low flow dimension, but a few streets have an extremely high flow dimension. This finding has a special implication for understanding traffic flows in urban systems. That is, always making those streets of an extremely high flow dimension through would significantly ease the traffic of an entire network system. It is important to note the two parts for the power-law tail with the San Francisco network, which is different from many others [15]. The distributions of the flow dimension appear to fit in to that of the degree or street connectivity distribution illustrated by our previous work [16,14].

The third finding is that the flow capacity of the topologies is larger than that of the random and regular counterparts (Table 2). This suggests that flow capacity can be a good indicator for determining whether or a real world network is a small world. This reminds us of the fact that the flow dimension resembles the clustering coefficient, and the flow length resembles the average path length. Therefore, the concept of flow capacity combines the initial two small world properties together into one formula, and it can be regarded as an alternative measure of network efficiency.

It should be noted that the above findings are made based on the primal topologies of urban street networks by taking the named streets as the nodes of the topologies, and eventually flow dimension and capacity are assigned to individual streets. However, we can also take the dual topologies of urban street networks by taking the junctions as the nodes of the topologies. This way the flow dimension and capacity can be computed and assigned to the individual junctions. Due to computational intensiveness, currently we are unable to obtain the flow capacity for the individual junctions of an entire network. However, our experiments based on partial networks illustrated the similar findings as above. Fig. 8 illustrates the geographic distribution of the flow capacity for the individual streets and junctions of the Sätra neighbourhood network within Gävle. They are represented respectively as the line thickness and dot size. We can remark that the flow capacity for streets fits quite well to that of junctions. Up to this point, we have seen how the flow dimension and capacity are defined and computed for both streets and junctions of the urban street networks.

The above findings have some universal value. This is particularly true for knowledge or innovation diffusion which often needs multiple disciplinary expertise, in order for a knowledge chunk to be spread. For example, with an organization, individuals' expertise differs from one to another, and those who share expertise (common nodes) are

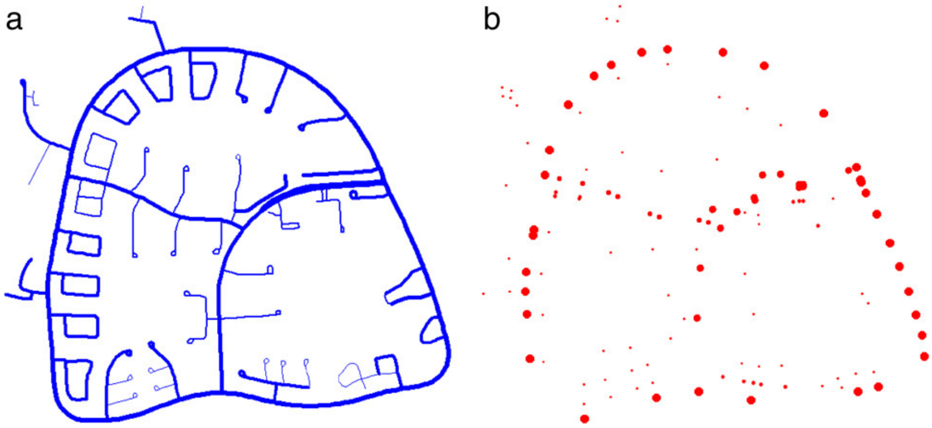

Fig. 8. Flow capacity for the individual streets (a) and junctions (b) of the Sätra neighbourhood.

likely to have a common language, and thus to have a knowledge chunk more quickly diffused from one to another. Those who have interdisciplinary background are likely to form m-cores for better knowledge diffusion. The concept of flow can help in differentiating from one organization network to another, or the individual persons' abilities in transferring knowledge within an organization.

5. Conclusion

This paper introduces the concept of multidimensional chain of connectivity or flow to characterize structural properties of urban street networks from both local and global levels. At the local level, it helps in differentiating between individual streets (or equivalently junctions) from one to another in terms of efficiency and it helps in identifying key structural streets or junctions. At the global level, it further illustrates the fact that an urban street network departs from its random and regular counterparts based on the single measure flow capacity. A major advantage of the flow capacity is that it takes multidimensional chain of connectivity into account while measuring efficiency of individual units or the entire network as a whole. In spite of the modelling capability, we must stress that the flow is a structural property, not the flows in reality such as vehicle and people flows. Whether the flow capacity can be a good indicator for real world flows is still an open question. This has implications for our future work.

Before any empirical verification of the concept and computation of flow, we tend to rely on its exploratory capability rather than possibilities of predicting real world flows. It helps in understanding and exploring traffic flows from a structural point of view. Taking the notional street network again for example, apparently it consists of two lattices: one to the left with four parallel streets at each direction crossing each other, and another to the right with two parallel streets crossed. From the structural point of view, the left lattice has a higher flow capacity than that of the right one. Thus it forms a gap or hole between the two lattices in terms of information flows. From the structural point of view, traffic jams are likely to occur between the two lattices. Of course, in reality traffic jams may not occur at all, if the number of vehicles is very low, or the vehicles are coordinated well. However the structural analysis based on the concept of flow capacity can help in indicating the possibility. We believe this is one of the major contributions of this paper besides the three major findings.

Acknowledgements

The author would like to thank Andrej Mrvar for his advice in using Pajek for partial computation and visualization with the study. The Munich dataset from the year 2000 was provided by NavTech, the San Francisco dataset from ESRI sample data, and the Gävle dataset by Gävle city. I am particularly grateful to Hong Zhang for her insightful discussions and comments.

Appendix. The matrixes associated with the notional street network

The street–street incidence matrix S can be represented by,

$$S = \begin{bmatrix} & s_1 & s_2 & s_3 & s_4 & s_5 & s_6 & s_7 & s_8 & s_9 & s_{10} & s_{11} \\ s_1 & 0 & 0 & 0 & 0 & 1 & 1 & 1 & 1 & 0 & 0 & 0 \\ s_2 & 0 & 0 & 0 & 0 & 1 & 1 & 1 & 1 & 0 & 0 & 0 \\ s_3 & 0 & 0 & 0 & 0 & 1 & 1 & 1 & 1 & 0 & 0 & 0 \\ s_4 & 0 & 0 & 0 & 0 & 1 & 1 & 1 & 1 & 0 & 0 & 0 \\ s_5 & 1 & 1 & 1 & 1 & 0 & 0 & 0 & 0 & 0 & 0 & 0 \\ s_6 & 1 & 1 & 1 & 1 & 0 & 0 & 0 & 0 & 0 & 0 & 0 \\ s_7 & 1 & 1 & 1 & 1 & 0 & 0 & 0 & 0 & 0 & 0 & 0 \\ s_8 & 1 & 1 & 1 & 1 & 0 & 0 & 0 & 0 & 1 & 1 & 0 \\ s_9 & 0 & 0 & 0 & 0 & 0 & 0 & 0 & 1 & 0 & 0 & 1 \\ s_{10} & 0 & 0 & 0 & 0 & 0 & 0 & 0 & 1 & 0 & 0 & 1 \\ s_{11} & 0 & 0 & 0 & 0 & 0 & 0 & 0 & 0 & 1 & 1 & 0 \end{bmatrix}. \tag{A.1}$$

From the matrix S, we can derive its flow matrix $FS = S * S'$ as follows:

$$FS = \begin{bmatrix} & s_1 & s_2 & s_3 & s_4 & s_5 & s_6 & s_7 & s_8 & s_9 & s_{10} & s_{11} \\ s_1 & 0 & 4 & 4 & 4 & 0 & 0 & 0 & 0 & 1 & 1 & 0 \\ s_2 & 4 & 0 & 4 & 4 & 0 & 0 & 0 & 0 & 1 & 1 & 0 \\ s_3 & 4 & 4 & 0 & 4 & 0 & 0 & 0 & 0 & 1 & 1 & 0 \\ s_4 & 4 & 4 & 4 & 0 & 0 & 0 & 0 & 0 & 1 & 1 & 0 \\ s_5 & 0 & 0 & 0 & 0 & 0 & 4 & 4 & 4 & 0 & 0 & 0 \\ s_6 & 0 & 0 & 0 & 0 & 4 & 0 & 4 & 4 & 0 & 0 & 0 \\ s_7 & 0 & 0 & 0 & 0 & 4 & 4 & 0 & 4 & 0 & 0 & 0 \\ s_8 & 0 & 0 & 0 & 0 & 4 & 4 & 4 & 0 & 0 & 0 & 2 \\ s_9 & 1 & 1 & 1 & 1 & 0 & 0 & 0 & 0 & 0 & 2 & 0 \\ s_{10} & 1 & 1 & 1 & 1 & 0 & 0 & 0 & 0 & 2 & 0 & 0 \\ s_{11} & 0 & 0 & 0 & 0 & 0 & 0 & 0 & 2 & 0 & 0 & 0 \end{bmatrix}. \tag{A.2}$$

More generally, the notational street network can be represented by a street–junction incidence matrix SJ:

$$SJ = \begin{bmatrix} & j_1 & j_2 & j_3 & j_4 & j_5 & j_6 & j_7 & j_8 & j_9 & j_{10} & j_{11} & j_{12} & j_{13} & j_{14} & j_{15} & j_{16} & j_{17} & j_{18} & j_{19} & j_{20} \\ s_1 & 1 & 0 & 0 & 0 & 1 & 0 & 0 & 0 & 1 & 0 & 0 & 0 & 1 & 0 & 0 & 0 & 0 & 0 & 0 & 0 \\ s_2 & 0 & 1 & 0 & 0 & 0 & 1 & 0 & 0 & 0 & 1 & 0 & 0 & 0 & 1 & 0 & 0 & 0 & 0 & 0 & 0 \\ s_3 & 0 & 0 & 1 & 0 & 0 & 0 & 1 & 0 & 0 & 0 & 1 & 0 & 0 & 0 & 1 & 0 & 0 & 0 & 0 & 0 \\ s_4 & 0 & 0 & 0 & 1 & 0 & 0 & 0 & 1 & 0 & 0 & 0 & 1 & 0 & 0 & 0 & 1 & 0 & 0 & 0 & 0 \\ s_5 & 1 & 1 & 1 & 1 & 0 & 0 & 0 & 0 & 0 & 0 & 0 & 0 & 0 & 0 & 0 & 0 & 0 & 0 & 0 & 0 \\ s_6 & 0 & 0 & 0 & 0 & 1 & 1 & 1 & 1 & 0 & 0 & 0 & 0 & 0 & 0 & 0 & 0 & 0 & 0 & 0 & 0 \\ s_7 & 0 & 0 & 0 & 0 & 0 & 0 & 0 & 0 & 1 & 1 & 1 & 1 & 0 & 0 & 0 & 0 & 0 & 0 & 0 & 0 \\ s_8 & 0 & 0 & 0 & 0 & 0 & 0 & 0 & 0 & 0 & 0 & 0 & 0 & 1 & 1 & 1 & 1 & 0 & 0 & 1 & 1 \\ s_9 & 0 & 0 & 0 & 0 & 0 & 0 & 0 & 0 & 0 & 0 & 0 & 0 & 0 & 0 & 0 & 0 & 1 & 0 & 1 & 0 \\ s_{10} & 0 & 0 & 0 & 0 & 0 & 0 & 0 & 0 & 0 & 0 & 0 & 0 & 0 & 0 & 0 & 0 & 0 & 1 & 0 & 1 \\ s_{11} & 0 & 0 & 0 & 0 & 0 & 0 & 0 & 0 & 0 & 0 & 0 & 0 & 0 & 0 & 0 & 0 & 1 & 1 & 0 & 0 \end{bmatrix} \tag{A.3}$$

From this street–junction incidence matrix, we can easily derive the above street–street incidence matrix S, i.e. $S = SJ * SJ'$ (Note: diagonal elements of S are set to 0). In the same fashion, we derive a junction–junction incidence matrix $J = SJ * SJ'$ (Note: diagonal elements of J are set to 0) as follows:

$$J = \begin{bmatrix} & j_1 & j_2 & j_3 & j_4 & j_5 & j_6 & j_7 & j_8 & j_9 & j_{10} & j_{11} & j_{12} & j_{13} & j_{14} & j_{15} & j_{16} & j_{17} & j_{18} & j_{19} & j_{20} \\
j_1 & 0 & 1 & 1 & 1 & 1 & 0 & 0 & 0 & 1 & 0 & 0 & 0 & 1 & 0 & 0 & 0 & 0 & 0 & 0 & 0 \\
j_2 & 1 & 0 & 1 & 1 & 0 & 1 & 0 & 0 & 0 & 1 & 0 & 0 & 0 & 1 & 0 & 0 & 0 & 0 & 0 & 0 \\
j_3 & 1 & 1 & 0 & 1 & 0 & 0 & 1 & 0 & 0 & 0 & 1 & 0 & 0 & 0 & 1 & 0 & 0 & 0 & 0 & 0 \\
j_4 & 1 & 1 & 1 & 0 & 0 & 0 & 0 & 1 & 0 & 0 & 0 & 1 & 0 & 0 & 0 & 1 & 0 & 0 & 0 & 0 \\
j_5 & 1 & 0 & 0 & 0 & 0 & 1 & 1 & 1 & 1 & 0 & 0 & 0 & 1 & 0 & 0 & 0 & 0 & 0 & 0 & 0 \\
j_6 & 0 & 1 & 0 & 0 & 1 & 0 & 1 & 1 & 0 & 1 & 0 & 0 & 0 & 1 & 0 & 0 & 0 & 0 & 0 & 0 \\
j_7 & 0 & 0 & 1 & 0 & 1 & 1 & 0 & 1 & 0 & 0 & 1 & 0 & 0 & 0 & 1 & 0 & 0 & 0 & 0 & 0 \\
j_8 & 0 & 0 & 0 & 1 & 1 & 1 & 1 & 0 & 0 & 0 & 0 & 1 & 0 & 0 & 0 & 1 & 0 & 0 & 0 & 0 \\
j_9 & 1 & 0 & 0 & 0 & 1 & 0 & 0 & 0 & 0 & 1 & 1 & 1 & 1 & 0 & 0 & 0 & 0 & 0 & 0 & 0 \\
j_{10} & 0 & 1 & 0 & 0 & 0 & 1 & 0 & 0 & 1 & 0 & 1 & 1 & 0 & 1 & 0 & 0 & 0 & 0 & 0 & 0 \\
j_{11} & 0 & 0 & 1 & 0 & 0 & 0 & 1 & 0 & 1 & 1 & 0 & 1 & 0 & 0 & 1 & 0 & 0 & 0 & 0 & 0 \\
j_{12} & 0 & 0 & 0 & 1 & 0 & 0 & 0 & 1 & 1 & 1 & 1 & 0 & 0 & 0 & 0 & 1 & 0 & 0 & 0 & 0 \\
j_{13} & 1 & 0 & 0 & 0 & 1 & 0 & 0 & 0 & 1 & 0 & 0 & 0 & 0 & 1 & 1 & 1 & 0 & 0 & 1 & 1 \\
j_{14} & 0 & 1 & 0 & 0 & 0 & 1 & 0 & 0 & 0 & 1 & 0 & 0 & 1 & 0 & 1 & 1 & 0 & 0 & 1 & 1 \\
j_{15} & 0 & 0 & 1 & 0 & 0 & 0 & 1 & 0 & 0 & 0 & 1 & 0 & 1 & 1 & 0 & 1 & 0 & 0 & 1 & 1 \\
j_{16} & 0 & 0 & 0 & 1 & 0 & 0 & 0 & 1 & 0 & 0 & 0 & 1 & 1 & 1 & 1 & 0 & 0 & 0 & 1 & 1 \\
j_{17} & 0 & 0 & 0 & 0 & 0 & 0 & 0 & 0 & 0 & 0 & 0 & 0 & 0 & 0 & 0 & 0 & 0 & 1 & 1 & 0 \\
j_{18} & 0 & 0 & 0 & 0 & 0 & 0 & 0 & 0 & 0 & 0 & 0 & 0 & 0 & 0 & 0 & 0 & 1 & 0 & 0 & 1 \\
j_{19} & 0 & 0 & 0 & 0 & 0 & 0 & 0 & 0 & 0 & 0 & 0 & 0 & 1 & 1 & 1 & 1 & 1 & 0 & 0 & 1 \\
j_{20} & 0 & 0 & 0 & 0 & 0 & 0 & 0 & 0 & 0 & 0 & 0 & 0 & 1 & 1 & 1 & 1 & 0 & 1 & 1 & 0
\end{bmatrix}. \tag{A.4}$$

Based on the junction–junction incidence matrix, we can further derive a flow matrix using the operation of $FJ = J * J'$ (Note: diagonal elements of FJ are set to 0)

$$FJ = \begin{bmatrix} & j_1 & j_2 & j_3 & j_4 & j_5 & j_6 & j_7 & j_8 & j_9 & j_{10} & j_{11} & j_{12} & j_{13} & j_{14} & j_{15} & j_{16} & j_{17} & j_{18} & j_{19} & j_{20} \\
j_1 & 0 & 2 & 2 & 2 & 2 & 2 & 2 & 2 & 2 & 2 & 2 & 2 & 2 & 2 & 2 & 2 & 0 & 0 & 1 & 1 \\
j_2 & 2 & 0 & 2 & 2 & 2 & 2 & 2 & 2 & 2 & 2 & 2 & 2 & 2 & 2 & 2 & 2 & 0 & 0 & 1 & 1 \\
j_3 & 2 & 2 & 0 & 2 & 2 & 2 & 2 & 2 & 2 & 2 & 2 & 2 & 2 & 2 & 2 & 2 & 0 & 0 & 1 & 1 \\
j_4 & 2 & 2 & 2 & 0 & 2 & 2 & 2 & 2 & 2 & 2 & 2 & 2 & 2 & 2 & 2 & 2 & 0 & 0 & 1 & 1 \\
j_5 & 2 & 2 & 2 & 2 & 0 & 2 & 2 & 2 & 2 & 2 & 2 & 2 & 2 & 2 & 2 & 2 & 0 & 0 & 1 & 1 \\
j_6 & 2 & 2 & 2 & 2 & 2 & 0 & 2 & 2 & 2 & 2 & 2 & 2 & 2 & 2 & 2 & 2 & 0 & 0 & 1 & 1 \\
j_7 & 2 & 2 & 2 & 2 & 2 & 2 & 0 & 2 & 2 & 2 & 2 & 2 & 2 & 2 & 2 & 2 & 0 & 0 & 1 & 1 \\
j_8 & 2 & 2 & 2 & 2 & 2 & 2 & 2 & 0 & 2 & 2 & 2 & 2 & 2 & 2 & 2 & 2 & 0 & 0 & 1 & 1 \\
j_9 & 2 & 2 & 2 & 2 & 2 & 2 & 2 & 2 & 0 & 2 & 2 & 2 & 2 & 2 & 2 & 2 & 0 & 0 & 1 & 1 \\
j_{10} & 2 & 2 & 2 & 2 & 2 & 2 & 2 & 2 & 2 & 0 & 2 & 2 & 2 & 2 & 2 & 2 & 0 & 0 & 1 & 1 \\
j_{11} & 2 & 2 & 2 & 2 & 2 & 2 & 2 & 2 & 2 & 2 & 0 & 2 & 2 & 2 & 2 & 2 & 0 & 0 & 1 & 1 \\
j_{12} & 2 & 2 & 2 & 2 & 2 & 2 & 2 & 2 & 2 & 2 & 2 & 0 & 2 & 2 & 2 & 2 & 0 & 0 & 1 & 1 \\
j_{13} & 2 & 2 & 2 & 2 & 2 & 2 & 2 & 2 & 2 & 2 & 2 & 2 & 0 & 4 & 4 & 4 & 1 & 1 & 4 & 4 \\
j_{14} & 2 & 2 & 2 & 2 & 2 & 2 & 2 & 2 & 2 & 2 & 2 & 2 & 4 & 0 & 4 & 4 & 1 & 1 & 4 & 4 \\
j_{15} & 2 & 2 & 2 & 2 & 2 & 2 & 2 & 2 & 2 & 2 & 2 & 2 & 4 & 4 & 0 & 4 & 1 & 1 & 4 & 4 \\
j_{16} & 2 & 2 & 2 & 2 & 2 & 2 & 2 & 2 & 2 & 2 & 2 & 2 & 4 & 4 & 4 & 0 & 1 & 1 & 4 & 4 \\
j_{17} & 0 & 0 & 0 & 0 & 0 & 0 & 0 & 0 & 0 & 0 & 0 & 0 & 1 & 1 & 1 & 1 & 0 & 0 & 0 & 2 \\
j_{18} & 0 & 0 & 0 & 0 & 0 & 0 & 0 & 0 & 0 & 0 & 0 & 0 & 1 & 1 & 1 & 1 & 0 & 0 & 2 & 0 \\
j_{19} & 1 & 1 & 1 & 1 & 1 & 1 & 1 & 1 & 1 & 1 & 1 & 1 & 4 & 4 & 4 & 4 & 0 & 2 & 0 & 4 \\
j_{20} & 1 & 1 & 1 & 1 & 1 & 1 & 1 & 1 & 1 & 1 & 1 & 1 & 4 & 4 & 4 & 4 & 2 & 0 & 4 & 0
\end{bmatrix}. \tag{A.5}$$

We can remark that both flow matrixes (A.2) and (A.5) have the same range of flow dimensions.

References

[1] R. Albert, A.-L. Barabási, Statistical mechanics of complex networks, Reviews of Modern Physics 74 (2002) 47–97.

[2] C. Alexander, A city is not a tree, Architectural Forum 122 (1+2) (1965) 58–62.

[3] L.A.N. Amaral, A. Scala, M. Barthelemy, H.E. Stanley, Classes of behaviour of small-world networks, in: Proceedings of the National Academy of Sciences, vol. 97, 2000, pp. 11149–11152.
[4] R.H. Atkin, Mathematical Structure in Human Affairs, Heinemann Educational Books, London, 1974.
[5] A.-L. Barabási, R. Albert, Emergence of scaling in random networks, Science 286 (5439) (1999) 509–512.
[6] M. Batty, A new theory of space syntax, CASA Working Paper, 2004. http://www.casa.ucl.ac.uk/working_papers/paper75.pdf.
[7] S. Boccalettia, V. Latorab, Y. Morenod, M. Chavez, D.-U. Hwang, Complex networks: Structure and dynamics, Physics Reports 424 (2006) 175–308.
[8] B. Bollobás, Random Graphs, Academic Press, London, 1985.
[9] F. Buckley, F. Harary, Distance in Graphs, Addison-Wesley, Redwood City, CA, 1990.
[10] K.Y. Degtiarev, System analysis: Mathematical modelling and approach to structural complexity measure using polyhedral dynamics approach, Complexity International (2000). http://www.complexity.org.au/.
[11] P. Erdös, A. Rényi, On the evolution of random graphs, Publications of the Mathematical Institute of the Hungarian Academy of Sciences 5 (1960) 17–61.
[12] P. Haggett, R.J. Chorley, Network Analysis in Geography, Edward Arnold, London, 1969.
[13] B. Jiang, C. Claramunt, Integration of space syntax into GIS: New perspectives for urban morphology, Transactions in GIS 6 (2002) 151–162.
[14] B. Jiang, Small world modelling for complex geographic environments, in: J. Portugali (Ed.), Complex Artificial Environments, Springer, Heidelberg, 2005, pp. 259–271.
[15] B. Jiang, A topological pattern of urban street networks: Universality and peculiarity, Physica A 384 (2007) 647–655.
[16] B. Jiang, C. Claramunt, Topological analysis of urban street networks, Environment and Planning B: Planning and Design, Pion Ltd 31 (2004) 151–162.
[17] V. Latora, M. Marchiori, Efficient behaviour of small-world networks, Physical Review Letters, 2001, 87.19, 198701-1-4.
[18] K. Lynch, The Image of the City, MIT Press, Cambridge, MA, 1960.
[19] S. Milgram, The small world problem, Psychology Today 2 (1967) 60–67.
[20] H.J. Miller, S.-L. Shaw, Geographic Information Systems for Transportation: Principles and Applications, Oxford University Press, Oxford, 2001.
[21] M.E.J. Newman, The structure and function of complex networks, SIAM Review 45 (2003) 167–256.
[22] M.E.J. Newman, D.J. Watts, Renormalization group analysis of the small-world network model, Physical Letters A 263 (1999) 341–346.
[23] M. Newman, A-L. Barabási, D.J. Watts, The Structure and Dynamics of Networks, Princeton University Press, Princeton, NJ, 2006.
[24] W. Nooy, A. Mrvar, V. Batagelj, Exploratory Social Network Analysis with Pajek, Cambridge University Press, Cambridge, 2005.
[25] S. Porta, P. Crucitti, V. Latora, The network analysis of urban streets: A dual approach, Physica A 369 (2006) 853–866.
[26] J. Scott, Social Network Analysis: A Handbook, SAGE Publications, London, 1991.
[27] D.J. Watts, S.H. Strogatz, Collective dynamics of 'small-world' networks, Nature 393 (1998) 440–442.